Chatter Identification in Milling of Titanium Alloy Using Machine Learning Approaches with Non-Linear Features of Cutting Force and Vibration Signatures

Viswajith S. Nair[1], Rameshkumar K.[2] and Saravanamurugan S.[3*]

[1,2,3*] *Department of Mechanical Engineering, Amrita School of Engineering, Amrita Vishwa Vidyapeetham, Coimbatore, Tamil Nadu, 641112, India*

sn_viswajith@cb.students.amrita.edu
k_rameshkumar@cb.amrita.edu
s_saravana@cb.amrita.edu

ABSTRACT

The generation of chatter during machining operations is extremely detrimental to the cutting tool life and the surface quality of the workpiece. The present study aims to identify chatter conditions during the end milling of Ti6Al4V alloy. Experimental modal analysis is carried out, and stability lobe diagrams (SLDs) are developed to identify machining parameters under stable and chatter conditions. Experiments are conducted to acquire cutting force and vibration signatures corresponding to machining conditions selected from the SLD. Non-linear chatter features, such as Approximate Entropy, Holder Exponent, and Lyapunov Exponent extracted from the sensor signatures, are used to build Machine Learning (ML) models to identify chatter using Decision Trees (DTs), Support Vector Machines (SVMs) and DT-based Ensembles. A feature-level fusion approach is adopted to improve the classification performance of the ML models. The DT-based Adaboost model trained using dominant non-linear features classifies chatter with an accuracy of 96.8%. The non-linear features extracted from the sensor signatures offer a direct indication of the chatter and are found to be effective in identifying the machining chatter with good accuracy.

1. INTRODUCTION

Titanium alloys are highly sought-after in aerospace, medical, chemical, automotive, and nuclear industries owing to their exceptional strength-to-weight ratio, corrosion resistance, biocompatibility, and high-temperature stability (G Welsch, R Boyer, 1994). Studies on the machinability of titanium alloys have revealed numerous issues associated with the process, such as high tool wear, high cutting temperatures, and built-up edge formation. Titanium alloy components often have thin walls with low stiffness, resulting in regenerative chatter during machining. The generation of chatter vibrations during machining operations is a major impediment to achieving good dimensional accuracy, high material removal rate, improved cutting tool life, and enhanced surface quality of machined components (Navarro-Devia et al., 2023; Tobias, 1961).

Stability Lobe Diagrams (SLDs) developed based on regenerative chatter theory can accommodate the complex non-linear behavior of chatter and clearly define the critical boundary between stable and unstable cutting conditions in terms of rotational speed and depth of cut (Altintaş & Budak, 1995; Tobias, 1961). By constraining the machining parameters to those in the stable region of the SLD, it is possible to prevent the occurrence of chatter. However, from a practical standpoint, on-line monitoring and control of the machining parameters to eliminate instabilities prior to their occurrence seem a more favorable action (Aggogeri et al., 2021). One of the drawbacks associated with the approach of constraining machining parameters to prevent chatter is that it sets limits on the machining capabilities. Furthermore, this approach may prove inadequate in addressing the variations and uncertainties in the machining process, such as tool wear, cutting forces fluctuations, and temperature effects, which may result in chatter under certain circumstances. Meanwhile, the online monitoring and control enables the machining system to adapt to changing conditions by dynamically adjusting the process parameters to prevent chatter. This approach may also be employed to simultaneously optimize the machining performance by selecting the best parameters for each situation. The challenge of identifying the process state/stability of automated machining systems can be effectively resolved through relevant sensor-based monitoring techniques (Navarro-Devia et al., 2023). Sensor signatures from various sources, including cutting force, voltage, acoustic, and

https://doi.org/10.36001/ijphm.2024.v15i1.3590

acceleration signals, can be effectively employed in an automated machining environment to predict critical factors like chatter vibrations, cutting forces, and surface topography of machined components (Kounta et al., 2022; Navarro-Devia et al., 2023). These signatures can be processed to filter out unnecessary information and extract the required signal data relevant to the process conditions. The sensor signals can be represented in time, frequency, or time-frequency domains, and relevant features of the signal data can be extracted using techniques such as Fourier analysis, wavelet transforms, and time-frequency analysis. The sensor signal features characterize and quantify significant signal parameters correlating with the process conditions. By utilizing Artificial Intelligence (AI) and Machine Learning (ML) techniques, it is possible to analyze the complex relationships between sensor signatures and machining process conditions. ML techniques such as Support Vector Machines (SVMs), Artificial Neural Networks (ANNs), and Decision Trees (DTs) have been employed for condition monitoring in machining systems.

Statistical measures of the sensor signals in the time, frequency, and time-frequency domains provide insights into the simple first-order characteristics of the signals and have been commonly utilized as linear features for chatter detection. However, these features may not adequately characterize complex phenomena, such as chaotic dynamics, self-similarity, fractal properties, or irregular fluctuations. Non-linear features such as fractal dimensions, Lyapunov exponent (LE), approximate entropy (ApEn), and Holder exponent (HE) that can describe the intricate patterns and complex phenomena present in the sensor signals have been employed to address this. The instabilities resulting from chatter are closely related to the irregularity and anti-persistent behavior of sensor signals. The ApEn statistic has been used as a non-linear measure to identify chatter by quantifying the regularity and complexity of vibration and sound signals (Chu et al., 2022; Chu & Xie, 2021; Pérez-Canales et al., 2011; Pincus, 1991). Pérez-Canales et al. (Pérez-Canales et al., 2011) determined that machining chatter could be correlated with the incremental increase of entropy of time-domain acceleration signals during milling. It was also found to be effective at identifying gradual as well as drastic changes in machining stability from a relatively small amount of data. HE has been employed as a measure of the degree of self-similarity to estimate the singularity of vibration, sound, and force signals for the purpose of monitoring machine tool conditions (Echelard & Lévy-Véhel, 2008; Mohanraj et al., 2021; Zhou et al., 2021; Zhou, Guo, et al., 2020; Zhou, Yang, et al., 2020). Studies show that the presence of singularities in sound and vibration waveforms, which generally vary slowly, can correspond to the presence of chatter vibrations. Research on condition monitoring using vibration signals by Mohanraj et al. (Mohanraj et al., 2021) concluded that prediction using HE and wavelet coefficient features provided better performance than conventional statistical features during milling. Different 'chaos quantifiers' such as the fractal dimension, correlation dimension, Kolmogorov entropy, and LE have also been employed to classify random and chaotic machine tool vibrations (Gredelj, 2021). The LE has been used to analyze the stability of the systems by identifying regions of instability and to characterize the chaotic behavior in time-domain sensor signals (Caesarendra et al., 2013; Guleria et al., 2022; Hamida et al., 2020; Pour, 2018; Rosenstein et al., 1993). Tran et al. (Tran et al., 2021) utilized the largest LE index of time-domain force signals to distinguish between stable and chatter conditions in milling. Guleria et al. (Guleria et al., 2022) employed extreme learning machine models developed using the features of the vibration signal modes identified using the largest LE to predict surface roughness during a turning process.

To improve the efficacy of detecting the process states during machining, recent studies have employed data fusion techniques that combine data from multiple sources (Gunatilaka & Baertlein, 2001; Krishnakumar et al., 2018; Navarro-Devia et al., 2023; Rameshkumar et al., 2022). In a recent study, Zhao et al.(Zhao et al., 2023) investigated an SVM-based model for the diagnosis of milling chatter using the non-linear features of energy entropy. The multi-signal fusion of cutting force and acceleration signal components was employed to improve the accuracy of the detection model. Ensemble methods have also been used in milling chatter prediction, where multiple models are ensembled to identify chatter states more accurately. Adaboost-SVMs have been employed with the fusion of vibration signal features to improve the accuracy and reliability of chatter detection (Wan et al., 2021). Ensemble models consisting of extreme learning machines have also been used for chatter detection in milling using features of cutting force and vibration signals (Liu et al., 2022).

There are limited studies on the utilization of chatter indexes and sensor fusion to assess the stability of machining processes in the literature. A bibliometric analysis of chatter diagnosis research over the past two decades, conducted using SCOPUS with a focus on keywords related to quantifiable chatter indexes and sensor fusion, identified fewer than 20 relevant research articles out of more than 175 publications on chatter diagnostic research. A large proportion of existing studies on chatter diagnosis seem to fall back on the use of statistical indicators. While these features are computationally efficient, they demonstrate limited generalization capabilities and exhibit poor adaptability to conditions beyond the initially trained parameters. Distinguishing chatter from other system vibrations may also prove difficult with these features. Quantifiable non-linear measures that can offer a direct indication of the chatter state, such as ApEn, HE, KE, and LE, are more favorable alternatives to statistical measures. Furthermore, these non-linear measures describe different characteristics of chatter, such as irregularity or chaos.

Considering both the irregularity and chaotic aspects of chatter may provide a more accurate description of the signal rather than considering them separately. The approach of fusing the different non-linear measures has been relatively unexplored and merits further investigation. The present work aims to address the challenge of accurately identifying and predicting the process state/stability during the milling of titanium alloy Ti6Al4V and expand on the area of chatter detection through ML using the feature-level fusion of ApEn, HE, and LE of cutting force and vibration signals.

2. METHODOLOGY

In this research, a multi-sensor feature-level fusion approach was suggested for the assessment of machining stability in milling using non-linear chatter features. The experimental methodology consisted of three parts: (a) Experimental Modal Analysis (EMA) to obtain the dynamic characteristics of the milling tool system needed to generate the stability lobes, (b) milling experiments on the titanium alloy Ti6Al4V to acquire the cutting force and vibration signatures at different stability conditions, and (c) signal processing, training, and testing of ML models to identify chatter. The overall methodology of the proposed study is depicted in Figure 1.

An experimental setup was established to study the dynamics of the end milling of Ti6Al4V alloy on a 'BMV 35 T12' vertical CNC milling machine, as shown in Figure 2(a). The impact test setup consisted of an accelerometer mounted onto the milling tool, an impact hammer, and a DAQ system. The 'Dytranpulse 5800B2' hammer, with a sensitivity of 22.5 mV/N and resonant frequency of 75kHz, was used to excite the system, and the resulting vibrations were acquired using the 'Dytran 3273 A2' piezo-electric accelerometer with a sensitivity of 100mV/g, to generate the Frequency Response Function (FRF) for constructing the SLD for the milling operation.

The equipment employed for the milling experiments on the Ti6Al4V alloy is shown in Figure 2(b). The milling tool used in the experiment was a four-flute tungsten carbide end mill tool of 10 mm diameter and 75 mm length. The 'Dytran 3273 A2' piezo-electric accelerometer mounted on the CNC spindle was used to acquire the machining vibration components at a sample rate of 25,000 Hz. The 'Kistler Type 9257B' dynamometer was attached to the work table of the milling machine to acquire cutting force components at a sampling rate of 25,000 Hz. The surface profile and roughness of the workpieces were measured using a Carl 'Zeiss E- 35B' profilometer.

3. THE DEVELOPMENT OF STABILITY LOBES FOR END MILLING OF TI6AL4V

3.1. Analytical Modeling of Stability Lobes

The SLDs provide valuable insight into the chatter characteristics of the machining operation on a theoretical basis. SLDs are specific to each machining system and vary for different combinations of machines, tools, and workpieces. SLDs utilize the FRF to evaluate the system response at various machining parameters. The FRF represents the transfer function containing valuable information about the system's dynamic response to external excitation. (Altintas, & Ber, 2001) The FRF quantifies the system behavior as a function of frequency, enabling analysis of vibrations, stability, and other dynamic characteristics.

The simplified 2-degree-of-freedom end milling process is depicted in Figure 3. The relationships governing the chatter behavior for the end milling process based on the average tooth angle approach (Altintaş & Budak, 1995) are provided in equations (1)–(8).

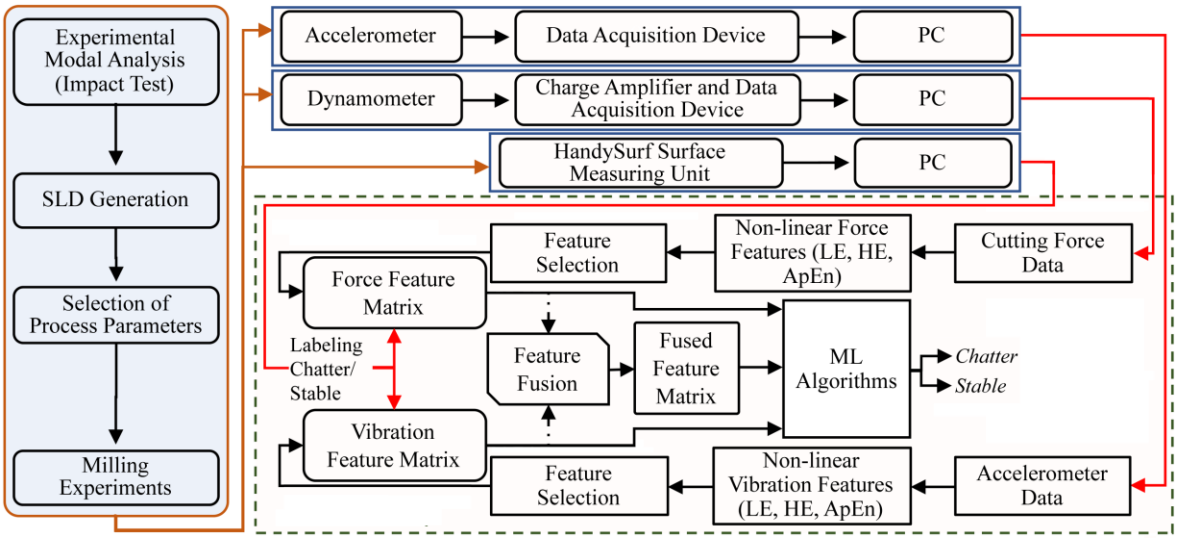

Figure 1. Methodology for development of ML model for chatter detection using non-linear features.

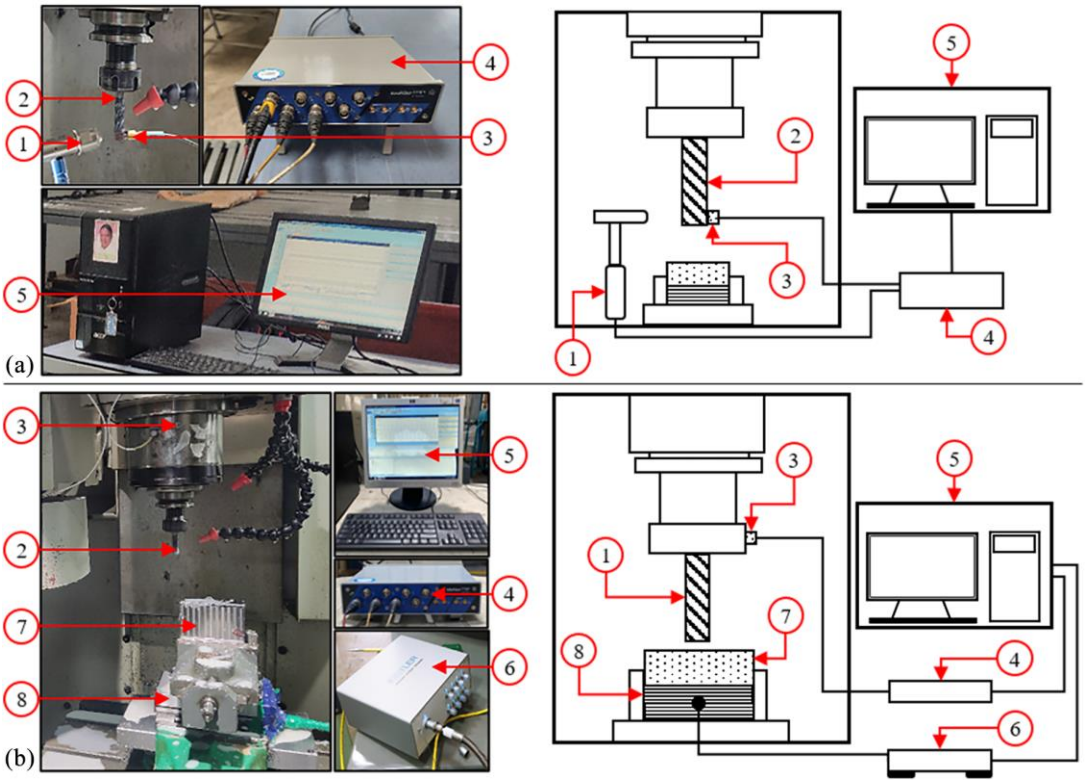

Figure 2. Experimental setups: (a) impact test for modal analysis, (b) milling experiments to acquire force and vibration signals. (Component description: 1.Impulse Hammer, 2.Tool, 3.Accelerometer, 4.DAQ, 5.PC, 6.LabAmp, 7. Ti6Al4V Specimen, 8.Dynamometer)

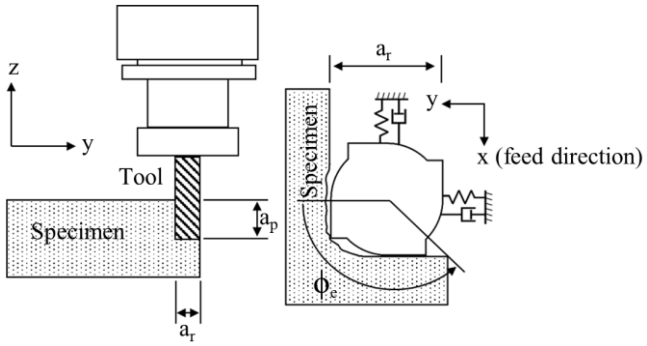

Figure 3. The modeling of the end milling process.

The axial depth of cut limit for stability,

$$a_{plim} = -\frac{1}{2K_s m A_{Rorient}} \quad (1)$$

Tooth passing period,

$$T = \frac{1}{\omega_c}\left(2\pi - \left(2cot\left(\frac{A_{Rorient}}{A_{Iorient}}\right)\right) + 2k\pi\right) \quad (2)$$

Spindle speed,

$$N = \left(\frac{60}{nT}\right) \quad (3)$$

The average number of teeth during the cut,

$$m = \frac{\phi_e - \phi_s}{\frac{360}{n}} \quad (4)$$

Here, K_s is the cutting coefficient, ω_c is the chatter frequency, k is the lobe number, a_r is the radial depth of cut, and n is the number of teeth. The ϕ_s and ϕ_e are the entry and exit angles of the tool during milling. For up milling, ϕ_s is zero degrees, and ϕ_e is calculated in degrees using the equation (5). The radius of the tool is denoted by r.

$$\phi_e = cos^{-1}\left(\frac{r - a_r}{r}\right) \quad (5)$$

For the down milling operation, ϕ_e is 180°, and ϕ_s is calculated using the equation (6).

$$\phi_s = 180 - cos^{-1}\left(\frac{r - a_r}{r}\right) \quad (6)$$

$A_{Rorient}$ and $A_{Iorient}$ are the real and imaginary components of the oriented FRF (FRF_{orient}). $A_{Rorient}$ and $A_{Iorient}$ are determined by calculating the FRF_{orient} for the current end milling process with 100% radial immersion from the FRFs in the x (feed direction) and y (direction of radial milling depth) directions using equation (7).

$$FRF_{orient} = \mu_x FRF_x + \mu_y FRF_y \quad (7)$$

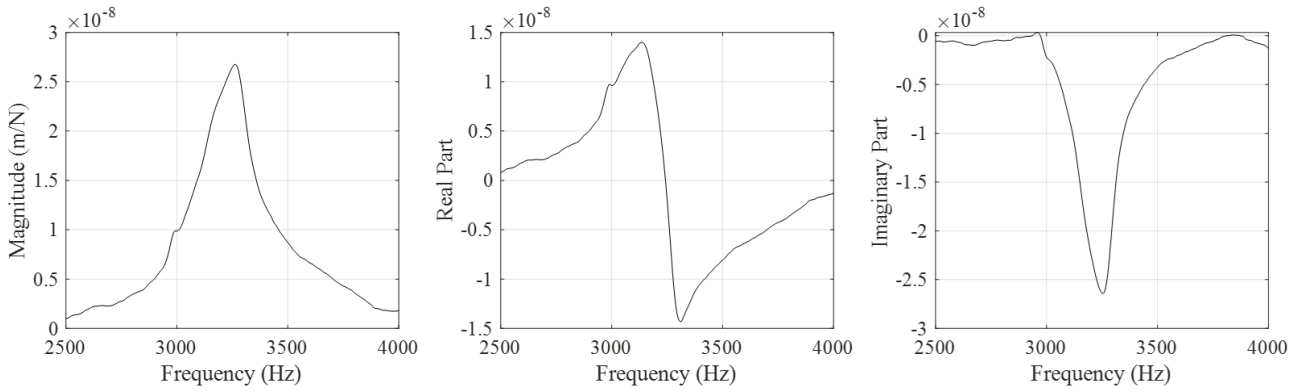

Figure 4. Plots of magnitude, real part, and imaginary part of FRF (in the feed direction) for milling tool system.

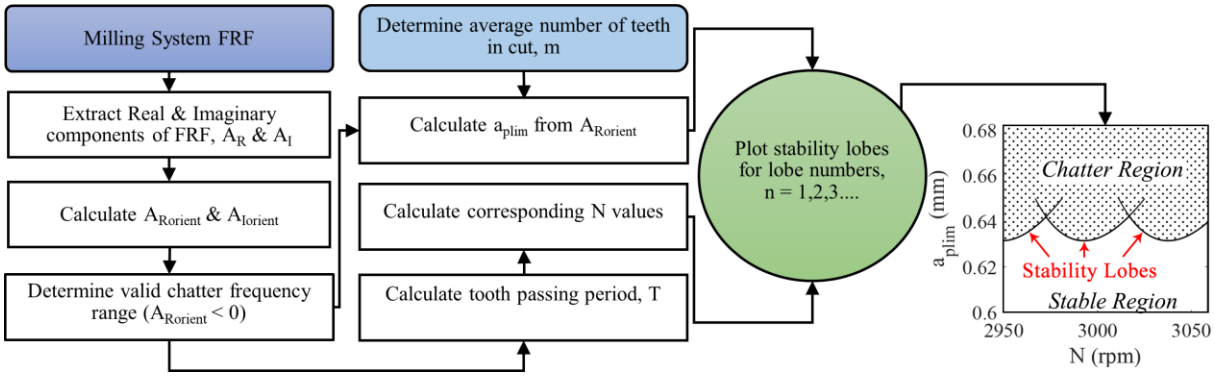

Figure 5. Flowchart for generating SLD.

The directional orientation factor μ_x is cos(β), where β is the force angle of the cutting force, and μ_y is zero, so equation (7) may be reduced to,

$$FRF_{orient} = FRF_x \cos(\beta) \quad (8)$$

3.2. The Development of SLD

The SLD for the end milling of the Ti6Al4V alloy was generated from the FRF and the governing equations (1)-(8). The FRF plots in the feed direction (FRF_x) are illustrated in Figure 4. It is noted that the principal natural frequency (ω_n) of the system obtained was 3252 Hz, corresponding to the maximum amplitude of the FRF. The real (A_R) and imaginary (A_I) components of FRF were also extracted for the construction of stability lobes. The range of frequencies above the obtained natural frequency was considered the chatter frequency range for the purpose of generating the stability lobes.

The cutting coefficient (K_s) was determined to be 1204.744 N/mm^2 through milling trials conducted in the stable domain by dividing the obtained average cutting forces by the product of the feed rate and axial depth of cut. The force angle (β) was similarly calculated analytically as per the method reported by Altintas and Ber (Altintas, & Ber, 2001) and was found to be 68°. The methodology for the SLD generation, as proposed by Schmitz & Smith (Schmitz & Smith, 2009), is depicted in Figure 5. The stability lobes indicated in the figure define the critical boundary between the stable and unstable machining parameters in terms of the optimum axial depth of cut (a_p) and spindle speed (N). Parameters below the lobe are selected for stable machining. The actual stability limits are presumed to be lower than the theoretical estimates.

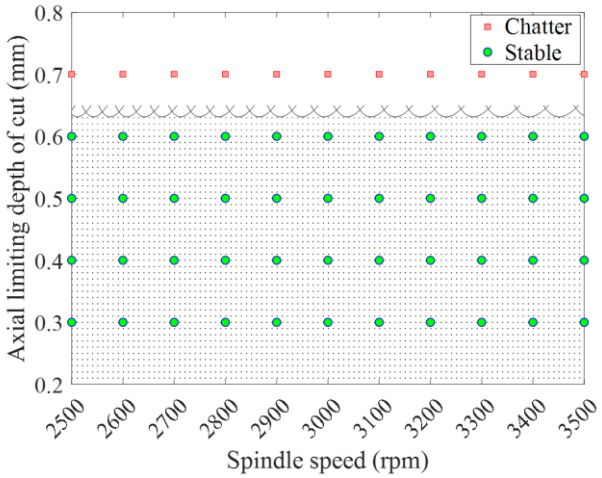

Figure 6. Experimental parameters selected from the SLD.

In order to process and analyze the signals from stable and chatter conditions at specific spindle speeds, a series of the axial depth of cut values from the stable and unstable regions of the SLD were selected, as shown in Figure 6. A constant feed rate (f_d) of 200 mm/min and a radial milling depth (a_r) of 1 mm were chosen to conduct the experiments.

4. VIBRATION AND CUTTING FORCE SIGNAL PROCESSING

4.1. Feature Extraction

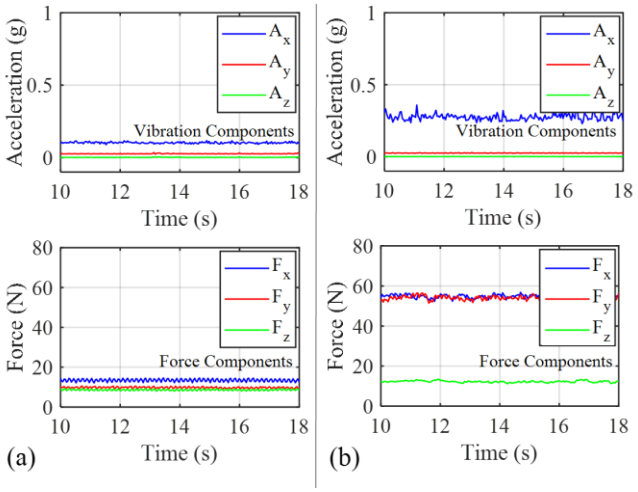

Figure 7. Time domain plots of vibration and force signals; (a) stable machining, (b) chatter.

The time domain cutting force and vibration signals recorded for the milling experiments corresponding to stable and chatter machining conditions are plotted in Figure 7. The force and vibration signal components in the radial feed direction (x-direction) were observed to be the most sensitive to the machining state. Meanwhile, the signal components perpendicular to the feed in the radial direction (y-direction) showed only slight responsiveness, and the signal components along the axis of the milling tool (z-direction) exhibited the least responsiveness. However, it is not easy to distinguish chatter and stable machining conditions in real time using sensor signatures alone.

In this study, LE, HE, and ApEn features were extracted from the time domain data to describe the state of the signals. The LE, HE, and ApEn features were extracted from the x, y, and z components of the force and vibration signals by considering a window size of 500. The computations for extracting LE, HE, and ApEn features are depicted in Figure 8, and the corresponding MATLAB code is provided in Appendix A. The extracted features were used to create three different ML datasets: the cutting force feature dataset, the vibration feature dataset, and the sensor-fusion dataset. The datasets were labeled as 'stable' or 'chatter' based on data from the SLD. The labeled feature datasets were used to train the ML models to identify the presence or absence of chatter during machining.

The feature-level fusion approach was adopted to improve the performance of the ML models. The fusion of data from multiple sensors serves to provide high signal-to-noise ratios, increased accuracy and reliability in the event of sensor breakdown, and reduced data ambiguity (Hall & Llinas, 1997). A total of 59,700 sets of vibration features and 59,700 sets of cutting force features were extracted from the stable and chatter machining conditions for training the ML models.

The statistical analysis of the extracted features in Figure 9 and Appendix B indicate that the non-linear features of chatter signals demonstrate greater complexity and variability than the more consistent stable signal features. Specifically, ApEn features of force signal components tend towards higher mean (μ) and standard deviation (σ) values in

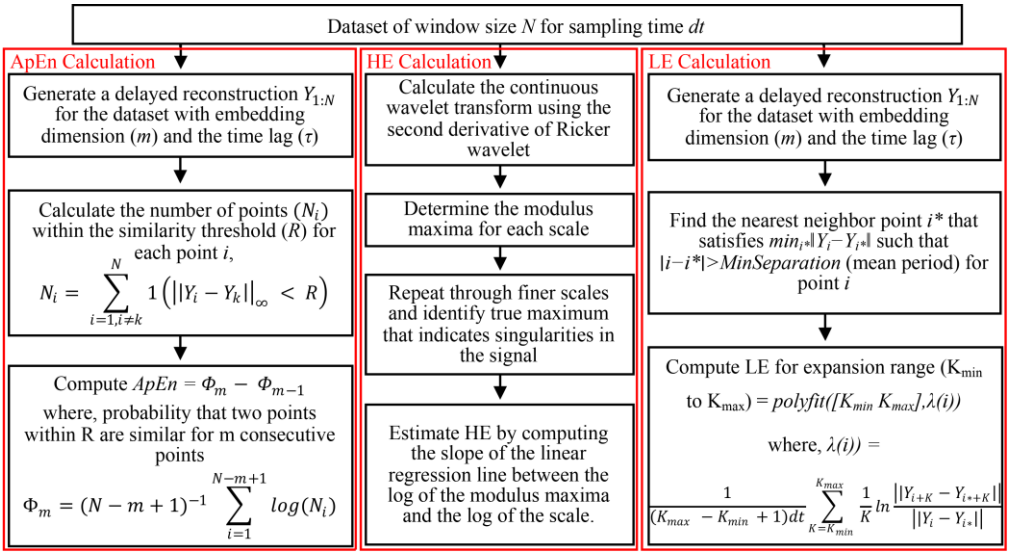

Figure 8. Computation of ApEn, HE, and LE features from time domain sensor signal data.

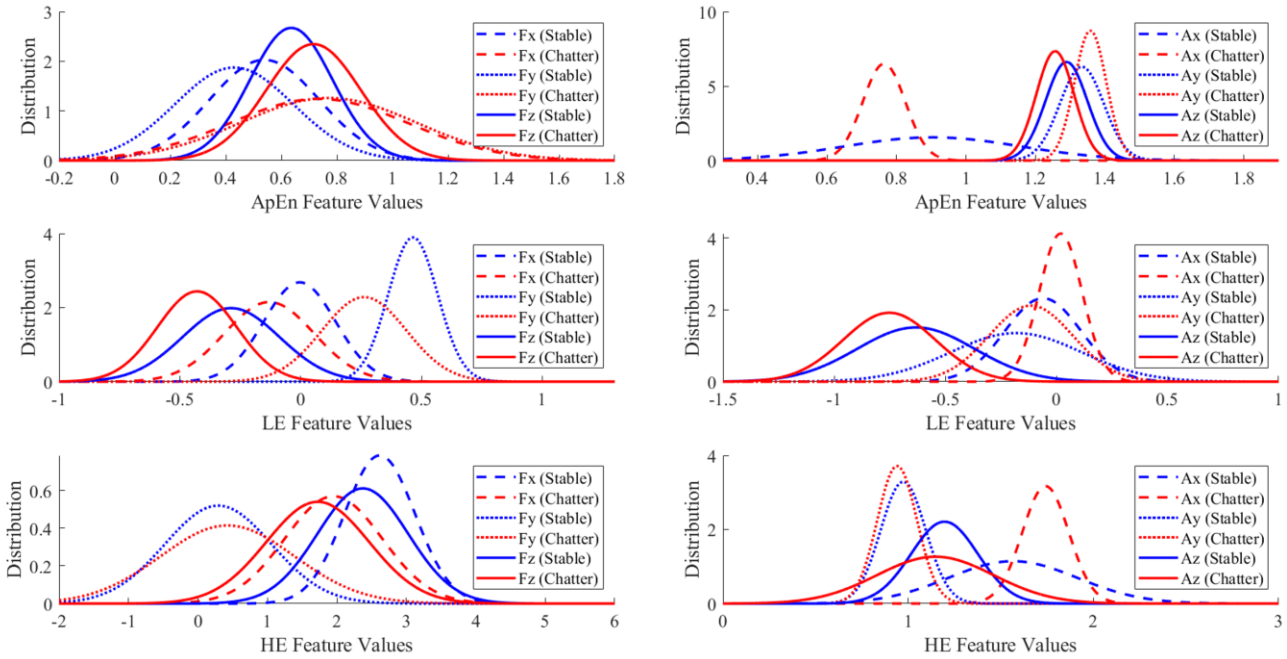

Figure 9. Statistics of extracted non-linear features: normal distribution curves.

the presence of chatter, indicating increased complexity and irregularity. Conversely, LE features of force signal components display lower μ values in relation to chatter. Notably, ApEn and LE features of the signal component A_x show the most pronounced differentiation between stable and chatter conditions. In contrast, F_x exhibits notable separability with HE features. Nonetheless, identifying distinct trends for chatter and stable conditions through the statistical analysis of these features remains challenging. The degree of separability varies among different features, with some trends being more prominent than others. Features of the force components prove to be more distinguishable than features of acceleration signals.

4.2. Statistical Classification based on Mahalanobis Distance

The statistical differences between the features enable some level of discrimination between chatter and stable features. The features were classified using a multivariate threshold based on the Mahalanobis distance (MD) metric (Hart et al., 2000). The MDs of the non-linear features from a reference distribution (denoted as R) were computed using equation (9), where F represents the set of non-linear features, and μ and Σ denote the mean and covariance of the reference distribution, respectively. The reference distribution was established using the stable condition features.

$$\mathrm{MD} = \sqrt{(\mathrm{F}-\mu)'\sum^{-1}(\mathrm{R}-\mu)} \qquad (9)$$

The threshold of MD demarcating the stable and chatter conditions was selected so as to minimize the instances of missed chatter conditions, which is of greater importance for the present scenario. The threshold, which covers over 80 % of the chatter data, was calculated using equation (10), where μ_c and σ_c are the mean and standard deviation of the MDs of chatter condition features. The thresholds were computed for force and vibration features separately, as well as for the fused features, as illustrated in Figure 10.

$$\text{Threshold} = \mu_c - \sigma_c \qquad (10)$$

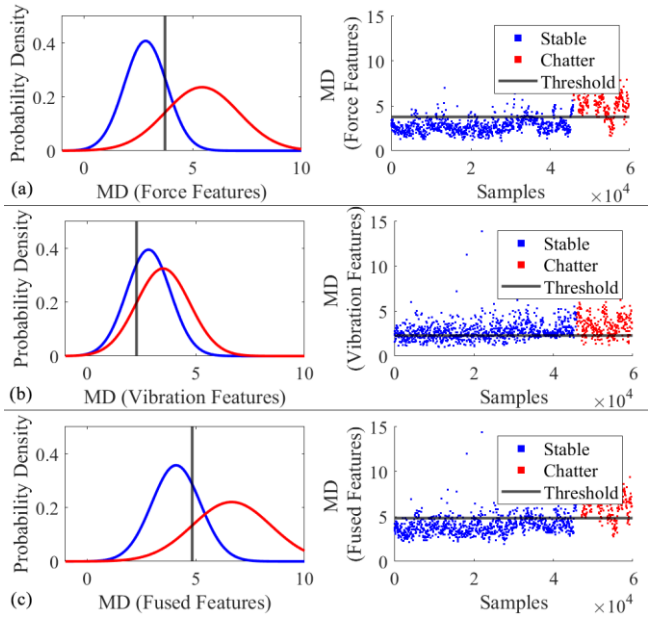

Figure 10. Thresholds based on MDs of (a) force features, (b) vibration features, and (c) fused features.

The performances of classifiers were evaluated using the confusion matrix, which represents the instances of true

stable, true chatter, false stable, and false chatter classifications made by the classifier model. It provided a thorough assessment of how well the model classifications conformed to actual stability conditions. The classifiers were evaluated with the help of various performance measures derived from the confusion matrix, such as accuracy, Cohen's Kappa, precision, recall, and F-score (Landis & Koch, 1977; Sokolova & Lapalme, 2009). The performance metrics of the statistical classification based on MD for the three feature datasets are tabulated in Table 1. The statistical classifier identified almost all the true chatter conditions owing to the threshold selection criteria, as signified by the high recall. However, this also resulted in the large misclassification of true stable conditions, as indicated by the low precision. The overall performance of the statistical classifier was also found to be lacking in the present scenario, as assessed through its F1 score and kappa metrics, despite the notable recall and accuracy. ML classification algorithms are explored in the subsequent sections to improve the overall classification performance.

Feature Set	***Performance Metrics***				
	Recall	***Precision***	***F1 Score***	***Kappa***	***Accuracy***
Vibration Features	82.69	26.03	39.60	0.06	41.05
Force Features	85.58	67.28	75.33	0.67	86.90
Fused Features	84.47	59.04	69.50	0.58	82.68

Table 1. Performance metrics of statistical classification.

5. MILLING STABILITY IDENTIFICATION USING ML

The DT, SVM, and ensemble learning algorithms were utilized with the feature datasets of vibration and force signals. The models were trained and tested using MATLAB R2022b software on a system equipped with an AMD Ryzen 5-2500U 2GHz CPU, 16 GB of RAM, and a 4 GB NVIDIA GTX 1050 GPU. The 5-fold cross-validation method was employed to train and test the DTs, SVMs, and DT-based ensemble models. DTs are prominent supervised ML classification algorithms widely used to solve complex problems by breaking them down into more minor, simpler decisions (Salzberg, 1994). The present study utilized DT models with various split criteria, such as Gini's Diversity Index (GDI), Maximum Deviance Reduction (MDR), and the twoing rule, to classify machining conditions.

SVM is another supervised learning algorithm that can be used for classification by identifying a hyperplane that separates the data points of different classes with maximum margin (Cortes & Vapnik, 1995). SVMs with linear, quadratic, and cubic kernel functions were trained in the study to identify the machining conditions from the cutting force and vibration features.

Ensemble methods are a type of ML algorithm that combines the strengths of multiple individual models to create a more robust and accurate prediction model while also reducing model complexity (Dong et al., 2020). Bagging and boosting ensemble methods based on DT algorithms were used to train classifiers to identify the machining conditions in the study. The primary boosting algorithm employed was Adaptive Boosting (AdaBoost), an ensemble algorithm that iteratively builds a robust classifier by combining multiple weak classifiers (Freund & Schapire, 1996). The basic idea behind it is to set the weights of classifiers and train the sample dataset in each iteration to ensure accurate predictions of unfamiliar observations. More weight is provided to the misclassified data in each iteration, which forces the algorithm to focus more on challenging sample datasets. By combining the results of these iterations, the algorithm builds a robust classifier that can accurately classify both simple and complex data, making it highly suitable for the present study.

6. RESULTS AND DISCUSSIONS

In the study, a grid search approach was employed for hyperparameter tuning to investigate the influence of model hyperparameters on the performance of the ML algorithms. Specifically, the DT models were fine-tuned by adjusting two key hyperparameters: the maximum number of splits and the split criterion. Meanwhile, the SVMs were tuned using

Algorithm	**Hyperparameter**	**Search Parameter Details**	**Optimal Results**
DT	***Maximum Splits***	4 to 100 (25 steps)	100
	Split Criterion	GDI, MDR, Twoing Rule	GDI
SVM	***Kernel Function***	Linear, Quadratic, Cubic	Cubic
	Box Constraint Level	1	-
	Kernel Scale	Auto	-
	Multiclass Method	One-vs-One	-
Ensemble	***Ensemble Type***	AdaBoost, Bagging	AdaBoost
	Base Learner	Decision Tree	-
	Number of Base Learner	6 to 30 (5 steps)	30
	Maximum Splits (Base Learner)	20	-
	Split Criterion (Base Learner)	GDI	-
	Learning Rate (AdaBoost)	0.1	-

Table 2. Hyperparameter settings for the ML models.

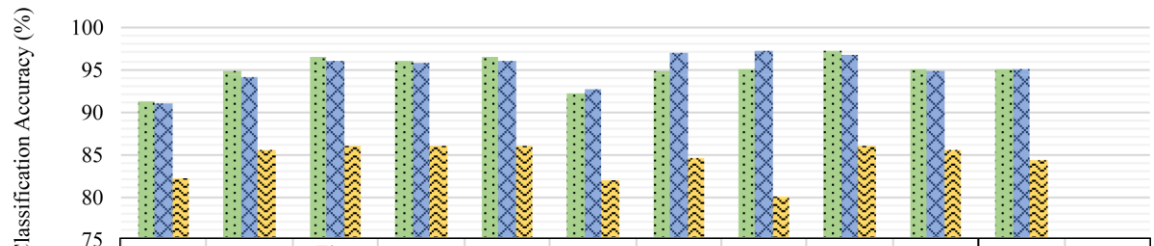

Dataset	Coarse DT	Medium DT	Fine DT: Twoing Rule	Fine DT: MDR	Fine DT: Gini	Linear SVM	Quad-ratic SVM	Cubic SVM	Adaboost	Bagging	Average	SD
	ML Model										*Statistics*	
Fused	91.2	94.7	96.5	95.9	96.6	92.2	94.9	95.1	97.3	95.1	95.0	1.8
Force	90.9	94.0	96.0	95.8	96.1	92.7	96.9	97.1	96.7	94.7	95.1	1.9
Vibration	82.2	85.5	86.0	86.0	86.0	82.0	84.6	79.9	85.9	85.6	84.4	2.1

Figure 11. Comparison of classification accuracies of the ML models.

Model	**Dataset**											
	Vibration				**Force**				**Fused**			
	Kappa	***Precision***	***Recall***	***F-score***	***Kappa***	***Precision***	***Recall***	***F-score***	***Kappa***	***Precision***	***Recall***	***F-score***
Coarse DT	0.34	81.52	99.29	89.54	0.72	91.28	97.37	94.23	0.73	91.47	97.60	94.44
Medium DT	0.51	85.04	98.41	91.24	0.83	95.26	97.00	96.12	0.85	95.34	97.88	96.59
Fine DT: Twoing Rule	0.53	85.65	98.23	91.51	0.53	96.62	98.25	97.43	0.90	96.96	98.56	97.75
Fine DT: MDR	0.53	85.67	98.15	91.49	0.53	96.34	98.26	97.29	0.88	96.45	98.32	97.38
Fine DT: GDI	0.53	85.64	98.16	91.47	0.53	96.62	98.29	97.45	0.90	97.24	98.38	97.81
Cubic SVM	0.35	83.01	92.37	87.44	0.92	97.10	99.16	98.12	0.85	94.47	99.40	96.87
Quadratic SVM	0.46	84.06	98.64	90.77	0.90	96.58	98.86	97.71	0.85	94.33	99.39	96.79
Linear SVM	0.37	82.34	97.42	89.25	0.79	93.06	98.08	95.50	0.76	92.02	98.33	95.07
Adaboost	0.52	85.17	98.74	91.46	0.97	97.25	98.52	97.88	0.92	97.72	98.76	98.24
Bagging	0.51	85.06	98.49	91.28	0.85	95.19	98.03	96.59	0.86	94.99	98.82	96.87

Table 3. Performance metrics of ML models.

different linear, quadratic, and cubic kernel functions. For the ensemble models, Adaboost and bagged tree algorithms were utilized with varying numbers of DT base learners, employing the best-performing GDI split criteria. The specific hyperparameter settings used for model training and the optimal hyperparameters identified using grid search are detailed in Table 2.

The comparisons of the overall performances of ML models are presented in Figure 11 and Table 3. The DT models are categorized according to their maximum number of splits as coarse DT (four splits), medium DT (twenty splits), and fine DT (one hundred splits). The SVM models are distinguished by their kernel function, and the ensemble models are labeled based on the employed ensemble type.

The force-based models were observed to have better performance compared to vibration-based models. In the DT models, increasing the maximum splits improved the performance, while the split criteria had minimal impact. The non-linear SVM models performed relatively better compared to linear SVM. The Adaboost models showcased better performance than the Bagged models, and increasing the number of base learners improved the model performance in both cases at the cost of increased model complexity.

It was observed that the feature-level fusion methodology could improve the performance of DT and ensemble models. The sensor-fused Adaboost model showcased the best performance with high accuracy, recall, precision, and F-score values. The model also had a kappa value extremely close to 1, indicating that the predictions made were incredibly close to the true conditions. The high precision signifies that a vast majority of the conditions identified as 'chatter' by the model were truly chatter conditions. The high recall indicates that the model is proficient in identifying almost all the true chatter conditions. A high recall is vital in the present scenario so as to not miss any of the instances of chatter. Misidentification of some stable instances as chatter is acceptable, whereas misidentification of chatter instances

as stable is highly detrimental to machining. The high F-score of the model confirms its superior performance, as it demonstrates that the model has attained a balance between precision and recall, making it effective in identifying most of the chatter conditions with minimal errors. The ML models were also observed to provide considerably better overall performance than the statistical classification using MD. Furthermore, feature selection was implemented on the best-performing algorithm to reduce computational costs and model complexity. A T-test (Livingston, 2004) was used to select dominant features from the feature-fused dataset for training the best-performing Adaboost ensemble model. Among the 18 features, the best 12 features (HE features of F_x, F_y, F_z, A_x, & A_y, ApEn features of F_x, F_y, A_x, & A_y, and LE features of F_x, F_z, & A_y), which have rich information on the process conditions, were chosen. The performances of Adaboost ensembles trained with all features and selected features are given in Table 4 and Figure 12. The findings demonstrate that feature selection offers improved computational efficiency and faster model training without compromising the model's classification accuracy.

Adaboost without Feature Selection		Predicted (%)		Adaboost with Feature Selection		Predicted (%)	
		Chatter*	***Stable****			***Chatter****	***Stable****
Actual (%)	***Chatter***	21.60	1.77	**Actual (%)**	***Chatter***	21.38	1.99
	Stable	0.95	75.68		***Stable***	1.19	75.44

Table 4. The confusion matrices of boosted ensemble models with and without feature selection.

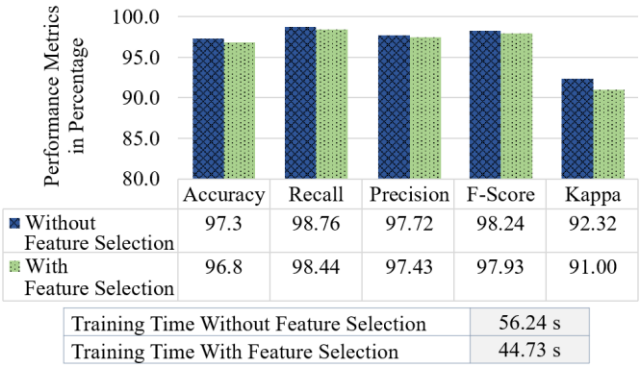

Figure 12. Effects of feature selection in the DT-based Adaboost model with feature-level fusion.

6.1. Validation of the Chatter Detection Model

The capability of the developed Adaboost model to detect chatter was validated using milling trials. Machining parameters for validation experiments were chosen from the SLDs for stable and chatter machining conditions. Fifty-five milling experiments were carried out on the Ti6Al4V alloy with different cutting speeds and axial depth of cuts. The force and vibration signals were acquired from the experiments, and the features were extracted and given as input to the best-performing DT-based ensemble model for classification. The surface profiles of the machined surfaces were obtained using the Carl 'Zeiss E- 35B' profilometer, and the surface roughness features were measured according to the 'ISO 4288' (International Standards Organization, 1996) standard, filtered using Gaussian filtering for a cutoff of 0.25 mm, a measuring length of 4 mm, and a measuring range of 20 μm.

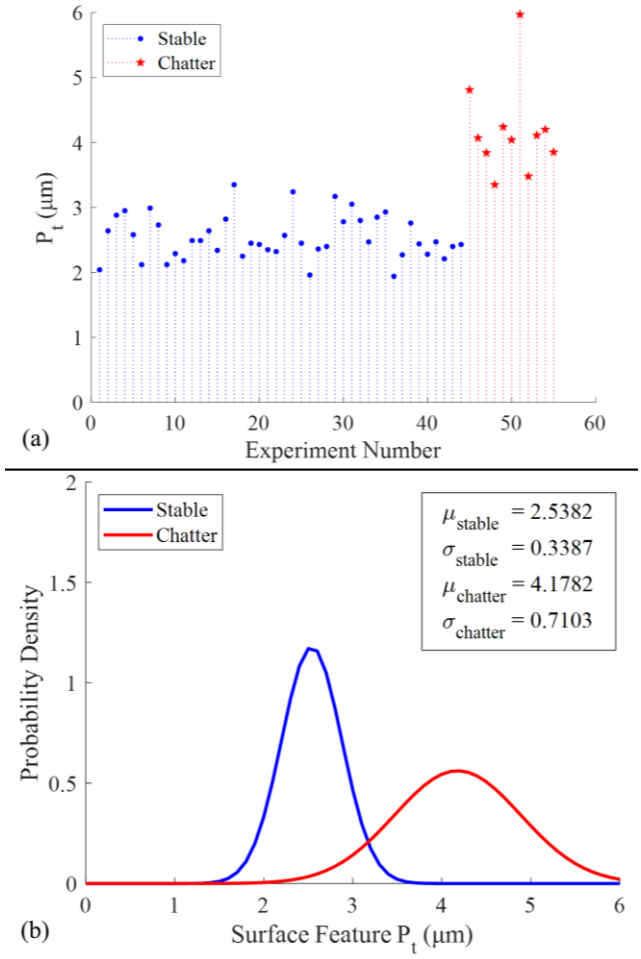

Figure 13. Statistical assessment of the surface feature: (a) progression of P_t with machining parameters, (b) normal distributions of the P_t corresponding to stability conditions.

The chip thickness variation corresponding to chatter can be correlated with the surface feature P_t (total profile peak height). This feature was taken as the primary consideration for chatter assessment, as given in Figure 13. The P_t values were observed to increase with the increase in the axial depth of cut for a given spindle speed (refer to Figure 13(a)). The fitted normal distributions for the P_t features corresponding to stable and chatter conditions are provided in Figure 13(b). For the stable points (as per the SLD), the P_t features obtained

through experiments presented a μ of 2.5382 with a tight σ of 0.3387.

In contrast, the chatter points had a much higher μ of 4.1782 and a wider σ of 0.7103. This indicates that the P_t values for stable and chatter conditions form distinct distributions with well-separated means. The wide σ observed in chatter conditions may be attributed to inherent variability associated with chatter. The conditions above the P_t value of 3.34 μm were observed to have a high probability of falling in the chatter region.

The vibration signals were further processed to obtain Moving Window Standard Deviation (MWSD) features for the stable and chatter machining conditions, as represented in the plots in Figure 14. The utilization of MWSD features of vibration signals, computed with a window size of 125, was chosen due to their effectiveness in revealing intricate patterns and trends in time-series data, which might remain concealed when analyzing the entire dataset (Nair et al., 2022). It is evident from the MWSD time domain plots that the vibration signature displays minimal amplitude variation during stable conditions. In contrast, during unstable/chatter conditions, there is a substantial increase in amplitude fluctuations. Notably, this amplitude variation is most pronounced in the A_x signal, indicative of chatter-induced vibrations in the feed direction, as depicted in Figure 14.

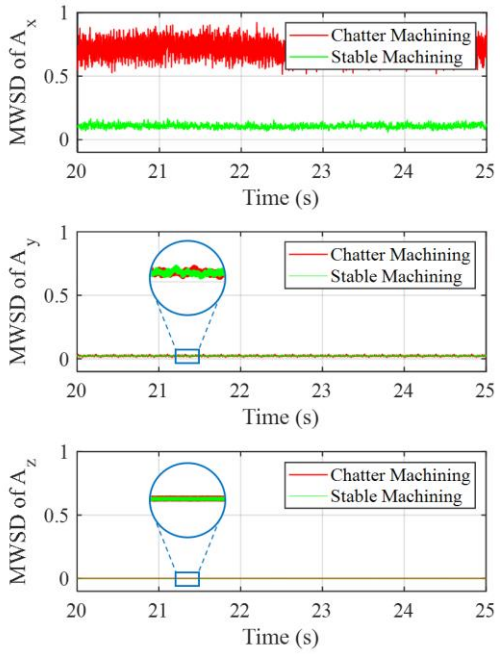

Figure 14. MWSD plots of machining vibration in stable and chatter machining conditions.

During stable machining, the mean MWSD values of the vibration amplitude signatures, A_x, A_y, and A_z, were observed to be 0.201, 0.001, and 0.023, respectively, with σ of 0.0720, 0.0001, and 0.0002. In contrast, when machined in chatter conditions, the mean MWSD values for A_x, A_y, and A_z signatures were determined to be 0.629, 0.001, and 0.024, respectively, with σ of 0.1710, 0.0003, and 0.007. The MWSD values and standard deviations of A_x and A_y signatures increased during chatter, indicating greater variability in the vibration amplitudes. Inspection of the machined surface produced under chatter conditions revealed the presence of chatter marks.

The true stable and chatter conditions were assessed through MWSD values, surface roughness features, and the visual inspection of the machined surface. A univariate threshold-based statistical classification using the MWSD feature of the A_x signal was used as a baseline to highlight the performance of the best-performing ML-based classifier model developed in the study. The performance measures of the univariate threshold-based classifier using the MWSD feature and the ML-based classifier using non-linear features are provided in Tables 5 and 6, respectively. In the case of the statistical classifier, the threshold separating the stable and chatter conditions was computed from the mean and standard deviation of the MWSDs of chatter condition A_x signals, using the relation established in equation (10). The threshold-based classification was found to be inefficient, with a low accuracy of 30.91 % and a Kappa of 0. It was also found to be lacking in terms of F1 score, precision, and recall. The comparison of the ML-based classification against the threshold-based statistical classification indicated that the performance of the ML model is superior across all the performance measures considered in the study. The validation results comparing the actual machining conditions and those predicted by the ML model are provided in Figure 15. It was observed that the ML model was able to classify 52 out of the 55 experimental conditions correctly as chatter or stable based on the non-linear features. The misclassifications were observed in conditions with lower speeds and axial depth of cuts close to the stability limits. It is also to be noted that no chatter conditions were misclassified as stable conditions.

Model Validation		**Model Prediction (%)**		
		Chatter*	***Stable****	
Actual (%)	***Chatter***	16.36	3.64	
	Stable	14.54	65.45	
Performance Metrics				
Recall	***Precision***	***F1 Score***	***Kappa***	***Accuracy***
81.82	20	32.14	0.00	30.91

Table 5. Performance of the threshold-based statistical classifier.

Model Validation		**Model Prediction (%)**		
		Chatter*	***Stable****	
Actual (%)	***Chatter***	20	0	
	Stable	5.45	74.55	
Performance Metrics				
Recall	***Precision***	***F1 Score***	***Kappa***	***Accuracy***
100	78.57	88	0.84	94.54

Table 6. Performance of the ML-based classifier.

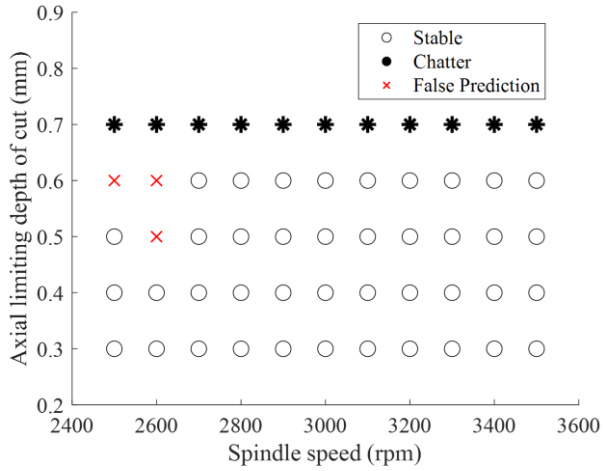

Figure 15. Results of model validation experiments.

The surface topographies of the machined surfaces for experimental trials 41 (stable), 42 (stable), 52 (chatter), and 53 (chatter) are provided in Figure 16. The validation experiments demonstrated that the SLDs and ML models developed in this study capture the dynamics of machining of Ti6Al4V alloy and can be implemented in a real-time machining environment.

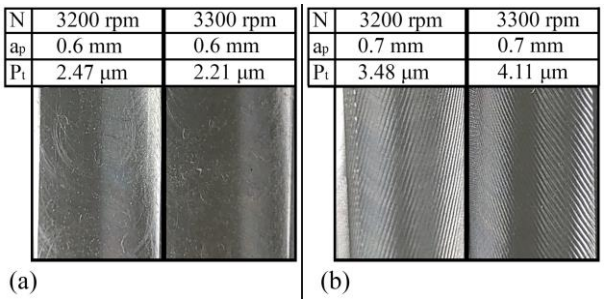

Figure 16. The surface topography of Ti-alloy workpieces: (a) under stable machining and (b) under unstable machining with noticeable chatter marks.

7. CONCLUSION

ML models were developed to identify stable and chatter conditions in the milling of Ti6Al4V alloy. SLDs were generated to understand the dynamics of machining and to arrive at the limiting values of the axial depth of cut and spindle speed for chatter-free milling. Experimental studies revealed that the surface roughness features and vibration characteristics correlated with the SLD conditions. Setting the spindle speed in the range of 2500 to 3500 rpm and axial depth of cut below 0.6 mm resulted in stable, chatter-free machining.

ML models were developed using force and vibration features separately and fused features of force and vibration. The proposed fusion methodology improved the classification accuracies of the DT and ensemble models by leveraging the complementarity of the non-linear features. All the feature-level fusion ML models proposed in the study using all features of vibration and force were able to identify the chatter condition with an accuracy of more than 91%. The DT-based Adaboost algorithm provided the highest classification accuracy of 97.3%. The Adaboost ensemble model utilized the variability of multiple base learners and an adaptive sampling strategy of assigning varying weights to challenging instances in the training data to reduce misclassifications. This may account for its superior performance.

The best-performing Adaboost model was trained using selected dominant features and identified the chatter conditions with an accuracy of 96.8%. Notably, the computational time required for training and testing the algorithm was reduced by 21%. Validation of the ML models using experimental data showed that the predicted conditions were in agreement with the actual chatter conditions, with an accuracy of 94.5% and a recall of 100%.

The developed ML models hold promise for adaptation in critical machining processes such as thin-wall machining for defense, aerospace, and medical applications. Subsequent research may investigate the feasibility of fine-tuning these models for application in diverse machining processes featuring distinct geometries, tools, and materials.

The proposed ML models were trained on stable and chatter states and did not address the transition behavior. The identification of the transition state may help to improve the reliability of the models further. Future studies may explore the development of an on-line chatter detection and control system.

REFERENCES

Aggogeri, F., Pellegrini, N., & Tagliani, F. L. (2021). Recent advances on machine learning applications in machining processes. *Applied Sciences*, *11*(18), 8764. https://doi.org/10.3390/app11188764

Altintas, Y., & Ber, A. (2001). Manufacturing Automation: Metal Cutting Mechanics, Machine Tool Vibrations, and CNC Design. *Applied Mechanics Reviews*, *54*(5), B84–B84. https://doi.org/10.1115/1.1399383

Altintaş, Y., & Budak, E. (1995). Analytical Prediction of Stability Lobes in Milling. *CIRP Annals*, *44*(1), 357–362. https://doi.org/10.1016/S0007-8506(07)62342-7

Caesarendra, W., Kosasih, B., Tieu, K., & Moodie, C. A. S. (2013). An application of nonlinear feature extraction - A case study for low speed slewing bearing condition monitoring and prognosis. *2013 IEEE/ASME International Conference on Advanced Intelligent Mechatronics: Mechatronics for Human Wellbeing, AIM 2013*, 1713–1718. https://doi.org/10.1109/AIM.2013.6584344

Chu, W. L., & Xie, M. J. (2021). Support-vector-machine-based sound and vibration signal processing for monitoring milling operations. *Proceedings of the 2021*

International Workshop on Modern Science and Technology, *2021*, 29–35. https://doi.org/10.19000/0002000099

Chu, W. L., Xie, M. J., Chang, Q. W., & Yau, H. T. (2022). Research on the Recognition of Machining Conditions Based on Sound and Vibration Signals of a CNC Milling Machine. *IEEE Sensors Journal*, *22*(7), 6364–6377. https://doi.org/10.1109/JSEN.2022.3150751

Cortes, C., & Vapnik, V. (1995). Support-vector networks. *Machine Learning*, *20*(3), 273–297. https://doi.org/10.1007/bf00994018

Dong, X., Yu, Z., Cao, W., Shi, Y., & Ma, Q. (2020). A survey on ensemble learning. *Frontiers of Computer Science*, *14*(2), 241–258. https://doi.org/10.1007/S11704-019-8208-Z/METRICS

Echelard, A., & Lévy-Véhel, J. (2008). Wavelet denoising based on local regularity information. *European Signal Processing Conference*. 10.1006/acha.2000.0299

Freund, Y., & Schapire, R. E. (1996). Experiments with a New Boosting Algorithm. *Proceedings of the 13th International Conference on Machine Learning*, 148–156. https://doi.org/10.1.1.133.1040

G Welsch, R Boyer, E. C. (1994). *Materials Properties Handbook: Titanium Alloys - ASM International*.

Gredelj, S. (2021). The Methodology of Distinguish Between Random and Chaotic Machine Tool Oscillations. *IOP Conference Series: Materials Science and Engineering*, *1208*(1), 012009. https://doi.org/10.1088/1757-899x/1208/1/012009

Guleria, V., Kumar, V., & Singh, P. K. (2022). Prediction of surface roughness in turning using vibration features selected by largest Lyapunov exponent based ICEEMDAN decomposition. *Measurement: Journal of the International Measurement Confederation*, *202*, 111812. https://doi.org/10.1016/j.measurement.2022.111812

Gunatilaka, A. H., & Baertlein, B. A. (2001). Feature-level and decision-level fusion of noncoincidently sampled sensors for land mine detection. *IEEE Transactions on Pattern Analysis and Machine Intelligence*, *23*(6), 577–589. https://doi.org/10.1109/34.927459

Hall, D. L., & Llinas, J. (1997). An introduction to multisensor data fusion. *Proceedings of the IEEE*, *85*(1), 6–23. https://doi.org/10.1109/5.554205

Hamida, Y., Naser, E., Karayel, D., & Kutlu, M. Ç. (2020). Investigation of Chaoticity of Vibrations in Machining. *Journal of Smart Systems Research*, *1*(1), 18–24. https://dergipark.org.tr/en/pub/joinssr/issue/64433/979663

Hart, P., Stork, D., & Duda, R. (2000). *Pattern classification* (2nd ed). John Wiley & Sons: Hoboken.

International Standards Organization (1996). Geometrical Product Specifications (GPS) - Surface texture: Profile method - Rules and procedures for the assessment of surface texture. In *ISO, ISO4288:1996(e). vol. ISO/IEC Directives Part 2, I. O. f. S. (ISO), (p. 14)*. Genève, Switzerland: International Standards Organization.

Kounta, C. A. K. A., Arnaud, L., Kamsu-Foguem, B., & Tangara, F. (2022). Review of AI-based methods for chatter detection in machining based on bibliometric analysis. *The International Journal of Advanced Manufacturing Technology 2022 122:5*, *122*(5), 2161–2186. https://doi.org/10.1007/S00170-022-10059-9

Krishnakumar, P., Rameshkumar, K., & Ramachandran, K. I. (2018). Feature level fusion of vibration and acoustic emission signals in tool condition monitoring using machine learning classifiers. *International Journal of Prognostics and Health Management*, *9*(1), 1–15. https://doi.org/10.36001/ijphm.2018.v9i1.2694

Landis, J. R., & Koch, G. G. (1977). The Measurement of Observer Agreement for Categorical Data. *Biometrics*, *33*(1), 159. https://doi.org/10.2307/2529310

Liu, W., Wang, P., & You, Y. (2022). Ensemble-Based Semi-Supervised Learning for Milling Chatter Detection. *Machines*, *10*(11), 1013. https://doi.org/10.3390/machines10111013

Livingston, E. H. (2004). Who was student and why do we care so much about his t-test? *Journal of Surgical Research*, *118*(1), 58–65. https://doi.org/10.1016/j.jss.2004.02.003

Mohanraj, T., Yerchuru, J., Krishnan, H., Nithin Aravind, R. S., & Yameni, R. (2021). Development of tool condition monitoring system in end milling process using wavelet features and Hoelder's exponent with machine learning algorithms. *Measurement: Journal of the International Measurement Confederation*, *173*, 108671. https://doi.org/10.1016/j.measurement.2020.108671

Nair, V., Krishnaswamy, R., & S., S. (2022). Chatter identification in turning of difficult-to-machine materials using moving window standard deviation and decision tree algorithm. *Journal of Ceramic Processing Research*, *23*(4), 503–510. https://doi.org/10.36410/jcpr.2022.23.4.503

Navarro-Devia, J. H., Chen, Y., Dao, D. V., & Li, H. (2023). Chatter detection in milling processes—a review on signal processing and condition classification. *The International Journal of Advanced Manufacturing Technology*, *125*(9–10), 3943–3980. https://doi.org/10.1007/s00170-023-10969-2

Pérez-Canales, D., Álvarez-Ramírez, J., Jáuregui-Correa, J. C., Vela-Martínez, L., & Herrera-Ruiz, G. (2011). Identification of dynamic instabilities in machining process using the approximate entropy method. *International Journal of Machine Tools and Manufacture*, *51*(6), 556–564. https://doi.org/10.1016/J.IJMACHTOOLS.2011.02.004

Pincus, S. M. (1991). Approximate entropy as a measure of system complexity. *Proceedings of the National Academy of Sciences of the United States of America*,

88(6), 2297–2301. https://doi.org/10.1073/pnas.88.6.2297

Pour, M. (2018). Determining surface roughness of machining process types using a hybrid algorithm based on time series analysis and wavelet transform. *The International Journal of Advanced Manufacturing Technology 2018 97:5*, *97*(5), 2603–2619. https://doi.org/10.1007/S00170-018-2070-2

Rameshkumar, K., Sriram, R., Saimurugan, M., & Krishnakumar, P. (2022). Establishing Statistical Correlation between Sensor Signature Features and Lubricant Solid Particle Contamination in a Spur Gearbox. *IEEE Access*, *10*, 106230–106247. https://doi.org/10.1109/ACCESS.2022.3210983

Rosenstein, M. T., Collins, J. J., & De Luca, C. J. (1993). A practical method for calculating largest Lyapunov exponents from small data sets. *Physica D: Nonlinear Phenomena*, *65*(1–2), 117–134. https://doi.org/10.1016/0167-2789(93)90009-P

Salzberg, S. L. (1994). C4.5: Programs for Machine Learning by J. Ross Quinlan. Morgan Kaufmann Publishers, Inc., 1993. *Machine Learning*, *16*(3), 235–240. https://doi.org/10.1007/bf00993309

Schmitz, T. L., & Smith, K. S. (2009). Machining dynamics: Frequency response to improved productivity. In *Machining Dynamics: Frequency Response to Improved Productivity*. Springer US. https://doi.org/10.1007/978-0-387-09645-2

Sokolova, M., & Lapalme, G. (2009). A systematic analysis of performance measures for classification tasks. *Information Processing and Management*, *45*(4), 427–437. https://doi.org/10.1016/j.ipm.2009.03.002

Tobias, S. A. (1961). Machine tool vibration research. *International Journal of Machine Tool Design and Research*, *1*(1–2), 1–14. https://doi.org/10.1016/0020-7357(61)90040-3

Tran, M. Q., Liu, M. K., & Tran, Q. V. (2021). Analysis of Milling Chatter Vibration Based on Force Signal in Time Domain. *Lecture Notes in Networks and Systems*, *178*, 192–199. https://doi.org/10.1007/978-3-030-64719-3_22

Wan, S., Li, X., Yin, Y., & Hong, J. (2021). Milling chatter detection by multi-feature fusion and Adaboost-SVM. *Mechanical Systems and Signal Processing*, *156*, 107671. https://doi.org/10.1016/j.ymssp.2021.107671

Zhao, M., Yue, C., & Liu, X. (2023). Research on milling chatter identification of thin-walled parts based on incremental learning and multi-signal fusion. *International Journal of Advanced Manufacturing Technology*, *125*(9–10), 3925–3941. https://doi.org/10.1007/s00170-023-10944-x

Zhou, C., Guo, K., & Sun, J. (2021). Sound singularity analysis for milling tool condition monitoring towards sustainable manufacturing. *Mechanical Systems and Signal Processing*, *157*, 107738. https://doi.org/10.1016/J.YMSSP.2021.107738

Zhou, C., Guo, K., Sun, J., Yang, B., Liu, J., Song, G., Sun, C., & Jiang, Z. (2020). Tool condition monitoring in milling using a force singularity analysis approach. *The International Journal of Advanced Manufacturing Technology 2019 107:3*, *107*(3), 1785–1792. https://doi.org/10.1007/S00170-019-04664-4

Zhou, C., Yang, B., Guo, K., Liu, J., Sun, J., Song, G., Zhu, S., Sun, C., & Jiang, Z. (2020). Vibration singularity analysis for milling tool condition monitoring. *International Journal of Mechanical Sciences*, *166*, 105254. https://doi.org/10.1016/J.IJMECSCI.2019.105254

APPENDIX A - MATLAB CODE FOR EXTRACTION OF NON-LINEAR FEATURES

```
clear all;
close all;
clc;

% Define file paths
raw_force_data_path = 'C:\Milling\Raw\Dynoware
Data\RAWForce_Exp_01.xlsx';

raw_accel_data_path = 'C:\Milling\Raw\Accelerometer
Data\RawAccel_Exp_01.lvm';

feature_data_path = 'C:\Milling\Features_Compiled\Non-
linear_Featureset_Exp_01.xlsx';

% Define time range and sampling rates
T1 = 5; % Start time in seconds
T2 = 25; % End time in seconds
sample_rate_force = 25000; % Sample rate of force signal
sample_rate_vibration = 25000; % Sample rate of
accelerometer signal

% Calculate sample indices for data extraction
force_data_samples = (T2 - T1) * sample_rate_force;
vibration_data_samples = (T2 - T1) *
sample_rate_vibration;
force_start_idx = (sample_rate_force * T1) + 3;
vibration_start_idx = (sample_rate_vibration * T1) + 23;
force_end_idx = (sample_rate_force * T2) + 2;
vibration_end_idx = (sample_rate_vibration * T2) + 22;

% Read data
force_data = readmatrix(raw_force_data_path, 'Range',
[force_start_idx 2 force_end_idx 4]);
accel_data = dlmread(raw_accel_data_path, '\t',
[vibration_start_idx 1 vibration_end_idx 3]);

% Extract individual force components
Fx = force_data(:, 1);
Fy = force_data(:, 2);
```

```
Fz = force_data(:, 3);

% Extract individual accelerometer components
Ax = accel_data(:, 1);
Ay = accel_data(:, 2);
Az = accel_data(:, 3);

% Initialize feature extraction parameters
window_size_force = 500;
window_size_accel = 500;
num_windows_force = floor(force_data_samples /
window_size_force);
num_windows_accel = floor(vibration_data_samples /
window_size_accel);

% Initialize feature matrix
Feat = zeros(num_windows_force + num_windows_accel,
18);

% Feature extraction from force and accelerometer signals
for i = 1:num_windows_force
    Feat(i, 1:9) = feature_extraction(Fx, Fy, Fz, (i - 1) *
window_size_force + 1, window_size_force);
end
for i = 1:num_windows_accel
    Feat(i, 10:18) = feature_extraction(Ax, Ay, Az, (i - 1) *
window_size_accel + 1, window_size_accel);
end

% Define header for the feature table
Header = {'ApEn Fx'; 'ApEn Fy'; 'ApEn Fz'; 'LE Fx'; 'LE
Fy'; 'LE Fz'; 'HE Fx'; 'HE Fy'; 'HE Fz'; 'ApEn Ax'; 'ApEn
Ay'; 'ApEn Az'; 'LE Ax'; 'LE Ay'; 'LE Az'; 'HE Ax'; 'HE
Ay'; 'HE Az'};

% Create a table of extracted features
Feat_Table = array2table(Feat, 'VariableNames', Header)

% Write the extracted features to a file
writetable(Feat_Table, feature_data_path);

% Function to extract features from a signal
function features = feature_extraction(X, Y, Z, start_idx,
win_size)
    subset_X = X(start_idx : start_idx + win_size - 1);
    subset_Y = Y(start_idx : start_idx + win_size - 1);
    subset_Z = Z(start_idx : start_idx + win_size - 1);
    features = [approximateEntropy(subset_X),
approximateEntropy(subset_Y),
approximateEntropy(subset_Z),
lyapunovExponent(subset_X),
lyapunovExponent(subset_Y),
lyapunovExponent(subset_Z), wtmm(subset_X),
wtmm(subset_Y), wtmm(subset_Z)];
end
```

APPENDIX B – STATISTICS OF NON-LINEAR FEATURES

Feature		Stability Condition	Statistics			
			Min	***Max***	***Mean***	***Standard Deviation***
ApEn	F_x	*Stable*	0.252	1.232	0.539	0.197
		Chatter	0.303	1.292	0.736	0.321
	F_y	*Stable*	0.151	1.225	0.430	0.213
		Chatter	0.277	1.330	0.770	0.316
	F_z	*Stable*	0.383	1.186	0.636	0.149
		Chatter	0.406	1.219	0.716	0.170
	A_x	*Stable*	0.363	1.461	0.904	0.256
		Chatter	0.522	1.051	0.764	0.061
	A_y	*Stable*	0.151	1.471	1.333	0.063
		Chatter	0.264	1.455	1.358	0.046
	A_z	*Stable*	0.059	1.461	1.289	0.060
		Chatter	0.912	1.420	1.257	0.054
HE	F_x	*Stable*	-0.560	0.550	-0.004	0.149
		Chatter	-0.642	0.377	-0.130	0.186
	F_y	*Stable*	0.000	0.806	0.465	0.102
		Chatter	-0.224	0.723	0.263	0.175
	F_z	*Stable*	-1.006	0.277	-0.288	0.201
		Chatter	-1.111	0.088	-0.429	0.164
	A_x	*Stable*	-0.565	0.412	-0.060	0.172
		Chatter	-0.284	0.402	0.019	0.097
	A_y	*Stable*	-0.831	1.104	-0.181	0.294
		Chatter	-0.948	0.956	-0.114	0.188
	A_z	*Stable*	-1.465	0.438	-0.632	0.264
		Chatter	-1.484	0.298	-0.752	0.208
LE	F_x	*Stable*	0.215	3.385	2.617	0.508
		Chatter	0.505	3.240	1.951	0.701
	F_y	*Stable*	-1.835	2.923	0.291	0.768
		Chatter	-2.065	2.890	0.425	0.963
	F_z	*Stable*	-2.264	3.317	2.374	0.653
		Chatter	0.326	3.054	1.724	0.739
	A_x	*Stable*	-0.860	2.407	1.565	0.349
		Chatter	1.211	2.269	1.742	0.126
	A_y	*Stable*	-3.223	1.830	0.973	0.121
		Chatter	0.453	1.526	0.940	0.107
	A_z	*Stable*	0.571	1.749	1.196	0.180
		Chatter	0.367	2.090	1.146	0.315